Enhanced confinement after multi-pellet injection into neutral beam injection heated plasmas in the stellarator TJ-II

K. J. McCarthy[1], I. García-Cortés[1], V. Tribaldos[2], D. Medina-Roque[1], N. Panadero[1], E. Ascasíbar[1], A. A. Chmyga[3], T. Estrada[1], J. Hernández-Sánchez[1], A. S. Kozachek[3], M. Liniers[1], P. Medina[1], M. A. Ochando[1], J. L. de Pablos[1], I. Pastor[1], C. Toledo[4], B. van Milligen[1] & TJ-II team[1]

[1]*Laboratorio Nacional de Fusión, CIEMAT, Madrid, Spain*
[2]*Universidad Carlos III de Madrid, leganes, Madrid, Spain*
[3]*Institute of Plasma Physics, NSC KIPT Kharkov, Ukraine*
[4]*Universidad Complutense de Madrid, Madrid, Spain*

Introduction

Pellet injection (PI) is widely used in magnetic confinement fusion (MCF) devices to achieve deep and efficient core plasma fuelling. Moreover, improved plasma performance, associated with such pellet fuelling, has been observed in numerous devices. A common characteristic of Pellet-induced Enhanced Confinement (PiEC) is a clear increase in post-injection energy confinement compared to discharges fuelled by gas puff and/or by recycling. In this work, we report how PI (using a single pellet or a train of pellets) gives rise to a PiEC in NBI-heated plasmas of the stellarator TJ-II. In particular, we review the evolution of selected plasma signals in the phase immediately after PI (< 5 ms) and along the ensuing time phase (5 ms to NBI switch off) once a PiEC has been developed and maintained. We also present and discuss initial neoclassical simulations for a PiEC phase after a single PI.

Experimental set-up

TJ-II is a 4-period medium-sized heliac-type stellarator with major radius of 1.5 m, a bean-shaped plasma cross-section with averaged minor radius, a, of ≤ 0.2 m, and on-axis magnetic field $B_0 \leq 1.1$ T. Plasmas, created using hydrogen, are heated using 2 gyrotrons operated at 53.2 GHz ($P_{ECRH} \leq 500$ kW, $t_{ECRH} \leq 300$ ms) and central electron densities, n_{e0}, and temperatures, T_{e0}, up to 1.7×10^{19} m^{-3} and 1.5 keV are attained, respectively. The corresponding central ion temperature, T_{i0}, is ≤ 90 eV. Additional heating is provided using 2 tangential NBI systems ($P_{NBI} \leq 1$ MW, $t_{NBI} \leq 120$ ms) operated in a counter/co-counter configuration (anti-parallel and/or parallel to the toroidal magnetic field direction), and n_{e0}, T_{e0}, and T_{i0} up to 10^{20} m^{-3}, 400 eV, and 130 eV, respectively, can be achieved. A pipe-gun type cryogenic PI, in which up to 4 hydrogen pellets can be created *in-situ*, and a gas propellant system for pellet acceleration, is installed. Its injection lines are equipped with light-gates and a microwave cavity detector to determine velocity (600 to 1200 m/s) and pellet mass (0.4 to $3\text{x}10^{19}$ H) [1]. Finally, its flexibility permits pre-programming pellet series (order & number of pellets) so separation times between pellets, Δt_p, can be ≥1 ms. In order to follow pellet ablation, Balmer H_α light emitted from the neutral cloud surrounding a pellet is recorded

using optical fibre based filtered diode systems installed outside nearby viewports. The TJ-II is also equipped with a large range of diagnostics, several of which are of interest here [2].

In this work, pellets are injected into the NBI-heated phase of TJ-II discharges (a = 0.192 m, B_0 = 0.95 T, V_{plasma} = 1.1 m^3). Plasmas, with hydrogen as the working gas, are created using ECRH, and once developed, additional heating is provided by one or both NBIs. In such instances, pellets penetrate well beyond the magnetic axis and, because of strong radial drifting of ablated material, post-ablation pellet particle deposition tends to occur in the plasma core [3].

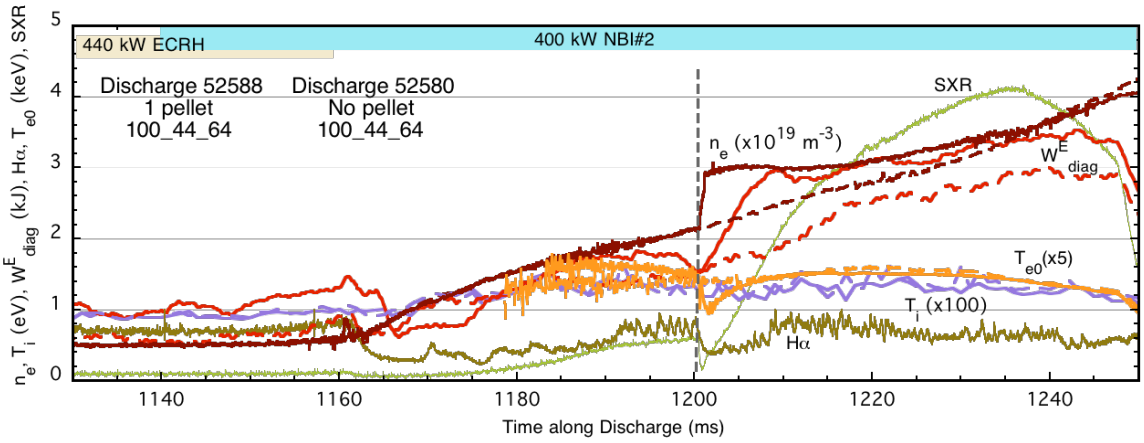

Figure 1: Signal traces (continuous lines) for several diagnostics along a TJ-II discharge into which a pellet is injected into the NBI heated phase at 1200 ms. Signals from a reference discharge are also shown (dashed lines). Immediately after PI, the line-averaged electron density increases and the core electron temperature decreases, the latter recovering quickly. Also, the stored diamagnetic energy, W^E_{diag} increases steadily before reaching a near constant value that is maintained until the heating is switched off (indicative of Enhanced Confinement).

Results

As an example, selected signal traces are shown in Figure 1 for a single PI into the NBI-heated phased of a TJ-II discharge. The pellet is fully ablated and deposited within ~1 ms. This is followed by an increase in n_e, a reduction in T_{e0} and reductions in H_α signal level, H_α fluctuations, and magnetic fluctuations (≤ 300 kHz but not shown), the latter being associated here with the rapid decrease in T_e [3]. Next, as n_e rises and T_{e0} recovers, the stored diamagnetic energy content, W^E_{diag}, is seen to rise to a plateau that is about 40% higher than W^E_{diag} of the reference discharge. Such behaviour is also seen when PI is performed at other times along the NBI phase of similar discharges. This indicates the existence of a bifurcation point where plasma is channelled towards an improved confinement phase, i.*e*., a pellet-induced enhanced confinement (PiEC) phase. Indeed, in this example, the energy confinement time, τ^E_{diag}, lengthens from ~7.6 ms to ~11 ms (where $\tau^E_{diag} = W^E_{diag} / (P_{abs} - dW^E_{diag}/dt)$. Here, absorbed NBI power, P_{abs}, is found using the FAFNER2 code which takes into account beam shine-through as well as CX and fast-ion losses [4], the former being measured also using

infrared cameras that view the NBI graphite beam dumps [5]. Next, in Figure 2, τ^{E}_{diag} are plotted for single, double and triple PI into similar and reference TJ-II discharges versus τ^{E}_{ISS04} for TJ-II. Here τ^{E}_{ISS04}, which includes a re-scaling factor of 0.5 for TJ-II [6], is energy confinement times predicted using the International Stellarator Scaling law [7]. It is apparent here that a new operation regime is attained by PI into the NBI-heated phase of TJ-II plasmas.

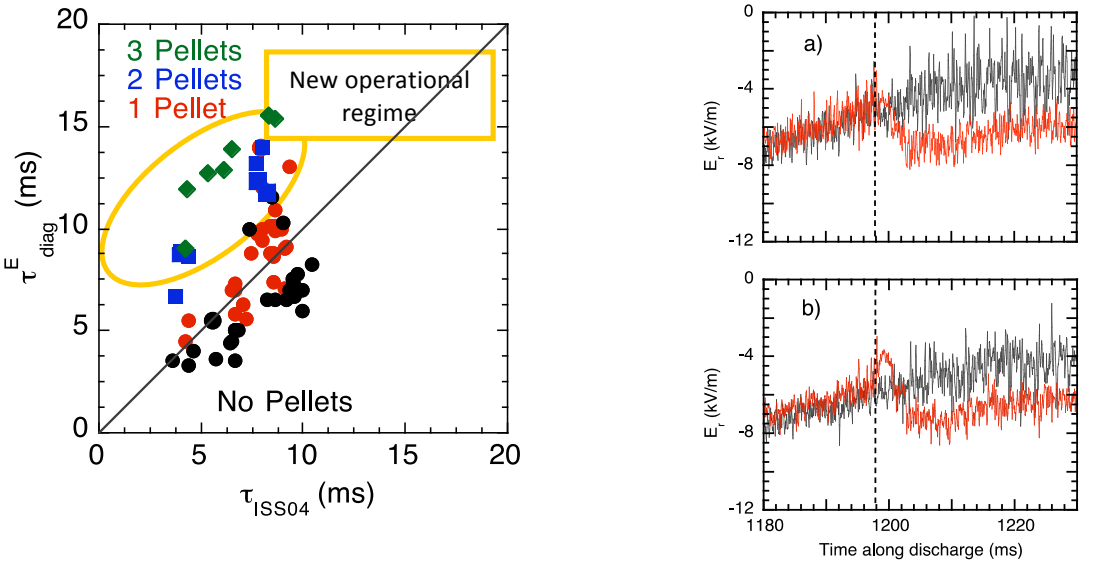

Figure 2: LHS: Experimental energy confinement times of assessed TJ-II discharges versus ISS04 times predicted for TJ-II NBI-heated discharges with re-scaling factor of 0.5 [6]. RHS: Temporal evolution of E_r and density fluctuation levels along two NBI-heated TJ-II discharges as measured by the 2-channel Doppler reflectometer at different radial positions, a) at $\rho = 0.75$ and b) at $\rho = 0.82$, for discharges with (red) and without PI (black).

Next, it is found for TJ-II PiEC regimes that plasma potential profiles, $\varphi(\rho)$, obtained by scanning a HIBP beam between low- and high-field side edges in periods of ~20.5 ms, becomes more negative after a PI. Similarly, the local φ at $\rho = 0.5$, as measured by a HIBP beam set at this radius, becomes more negative and remains so until discharge termination. The HIBP current, I_{HIBP}, also reduces immediately after PI, this attenuation being due to the increased post-injection density, and remains so until the discharge ends. Furthermore, the root mean squares of both I_{HIBP} and φ reduce immediately after PI and remain reduced before increasing slightly at ~15 ms later, albeit to values lower than pre-PiEC values. Finally, when the HIBP beam is set to measure at $\rho = 0.75$, a rise to a slightly less negative φ is observed for a brief period after PI. However, within a few milliseconds, φ becomes more negative than before PI and φ fluctuations higher than pre-PI one are observed. In contrast, I_{HIBP} shows no clear changes in terms of absolute value or fluctuations.

In a 2nd set of discharges, PIs are made into NBI-heated plasma created in the magnetic configuration with $\iota_0/2\pi = 1.5$ and the evolution of the radial electric field, E_r, is followed at

two radial positions in the edge region, ρ = 0.75 and 0.82, using the 2-channel Doppler reflectometer. It is seen, Figure 2, how, at ρ = 0.75, E_r become more negative immediately after PI, when compared to a discharge without PI, and remains so for the remainder of the discharge. In the case of ρ = 0.82, E_r become more positive for several milliseconds become more negative. In contrast, electron density fluctuations levels appear to be unaffected for both channels by a PI.

Finally, neoclassical simulations [8] made for discharges #52580 and #52588, using Thomson Scattering n_e and T_e profiles collected at 1230 ms in Figure 1, indicate that PI induced changes in plasma profiles should result in more negative ambipolar E_r, in agreement with HIPB measurements, and in reductions in particle and heat fluxes, these being consistent with improved confinement. See Figure 3. However, the connection between more a negative E_r, and its shear around ρ = 0.5, and observed reductions in magnetic & plasma potential fluctuations requires further study. Nonetheless it is possible to say that, during a PiEC, changes occur in E_r in the region ρ ≤0.8. However, the location of the region where maximum changes occur may depend on n_e and magnetic configuration. Furthermore, it appears that the reduction of fluctuations may be limited to regions close to the core, *e.g.*, at ρ = 0.5, since HIBP and Doppler do not detect reduced fluctuation levels in the range ρ = 0.7 to 0.85.

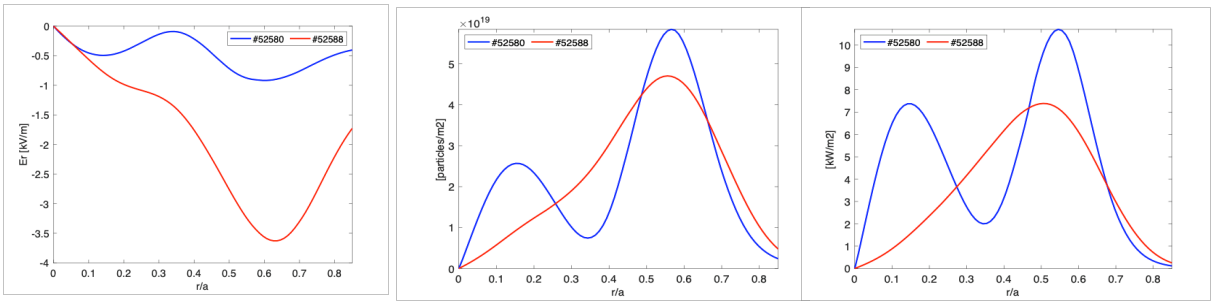

Figure 3. Neoclassical simulations made at t = 1230 ms for the TJ-II discharges in Figure 1. Left: Radial electric field, Centre: Particle Flux, and Right: Heat Flux.

This work has been carried out within the framework of the EUROfusion Consortium, funded by the European Union via the Euratom Research and Training Programme (Grant Agreement No 101052200 - EUROfusion). Views and opinions expressed are however those of the author(s) only and do not necessarily reflect those of the European Union or the European Commission. Neither the European Union nor the European Commission can be held responsible for them. In addition, it is partially financed by grants from the Spanish Ministerio de Ciencia e Innovación (PID2020-116599RB-I00). The authors acknowledge the contributions to data collection, analysis and interpretation made by A. Melnikov, M. Drabinskiy, L. G. Eliseev, and P. Khabanov.

[1] S K Combs *et al*, Fusion Sci Tech. 64 (2013) 513.
[2] K J McCarthy *et al*, J. Instrum. 16 (2021) C12026.
[3] K J McCarthy *et al*, Nucl. Fusion 61 (2021) 076014.
[4] J Guasp *et al*, Informes Técnicos Ciemat 1050. Dec 2004.
[5] M Liniers et al, J. Instrum. 14 (2019) C09021.
[6] M A Ochando *et al*, 41st EPS Conf (2014) P2.074.
[7] H Yamada *et al*, Nucl. Fusion 45 (2005) 1684.
[8] V Tribaldos *et al*, Phys Plasmas 18 (2011) 102507.